

# **Reduction of Resistivity in Cu Thin Films by Partial Oxidation: Microstructural Mechanisms**

By

Michael F. Toney, et al.

*Submitted to Applied Physics Letters*

*Stanford Linear Accelerator Center, Stanford University, Stanford, CA 94309*

---

Work supported by Department of Energy contract DE-AC03-76SF00515.

APPLIED PHYSICS LETTERS

Reduction of Resistivity in Cu Thin Films by Partial Oxidation: Microstructural Mechanisms

Walter L. Prater, Emily L. Allen, and R. Lawrence Comstock

*Chemical and Materials Engineering Dept., San Jose State University, One Washington Square, San Jose, CA 95192*

Wen-Y. Lee

*Hitachi Global Storage Technologies, 5600 Cottle Road, San Jose, CA 95193*

Michael F. Toney

*Stanford Synchrotron Radiation Laboratory, Stanford Linear Accelerator Center, 2575 Sand Hill Road, Menlo Park, CA 94025*

Jonathan Daniels and Jonathan Hedstrom

*IBM Almaden Research Center, 650 Harry Road, San Jose, CA 95120*

We report the electrical resistance and microstructure of sputter deposited copper thin films grown in an oxygen containing ion-beam sputtering atmosphere. For films thinner than 5 nm, 2-10% oxygen causes a decrease in film resistance, while for thicker films there is a monotonic increase in resistivity. X-ray reflectivity measurements show significantly smoother films for these oxygen flow rates. X-ray diffraction shows that the oxygen doping causes a refinement of the copper grain size and the formation of cuprous oxide. We suggest that the formation of cuprous oxide limits copper grain growth, which causes smoother interfaces, and thus reduces resistivity by increasing specular scattering of electrons at interfaces.

Recently, magnetic recording areal densities have increased at a compound annual growth rate of nearly 100%<sup>1</sup>, which has led to a demand for higher readback sensitivity from the spin-valve sensors used in recording technology. One approach to achieve higher sensitivity is the enhancement of the spin-valve giant magnetoresistance (GMR) through an increase in specular electron scattering at interfaces<sup>1-3</sup> in the spin valve. This enhancement partially results from an increased mean free path of majority spin-polarized electrons through reflection at interfaces, which increases  $\Delta R/R$  by increasing  $\Delta R$  and/or decreasing the resistance (R). This has been achieved by introducing oxygen during thin film deposition.<sup>4,6</sup> While oxygen has been reported to produce smoother interfaces, the role of oxygen is still a matter of debate and oxygen has been variously reported to decrease interlayer mixing of the spin-valve stack,<sup>7</sup> suppress the diffusion scattering coefficient,<sup>8</sup> or act as a surfactant.<sup>9,10</sup> The control of the oxygen concentration is critical to the success of the specular enhancement by influencing the film microstructure.<sup>11</sup> The goal of this paper is to understand the microstructural mechanism behind the reduced resistivity of partially oxidized copper thin films.

We show that 6 to 10% oxygen in the sputtering atmosphere sharply reduces the Cu film resistivity due to the formation of smoother interfaces, which cause an increase in specular electron scattering. The smoother interfaces result from the formation of small cuprous oxide particles in the Cu films that limit the copper grain growth.

The copper films were deposited in an ion-beam sputtering system using xenon gas mixed with oxygen at a total flow rate of 0.55 standard cubic centimeters (sccm). The oxygen percentage was varied from 0 to 60%. The base pressure was  $1.8 \times 10^{-8}$  Torr and temperature was 298 K. Copper film thicknesses ranged from 2.5 to 100 nm determined from the sputtering rate and the films were deposited on 25 mm diameter glass substrates. An in-line 4-point probe measured sheet resistance. The X-ray

reflectivity measurements were conducted using Cu  $K_{\alpha 1}$  radiation from a rotating anode x-ray generator. Slits were used for collimation.<sup>12</sup> X-ray diffraction (XRD) was conducted at the National Synchrotron Light Source, beamline X20C, using 1 milliradian Soller slits for collimation.<sup>13</sup> A grazing incidence geometry was used to reduce background scattering from the glass substrate.

Figure 1 shows resistivity data for the 4.5, 5, 10 and 100 nm films and illustrates four trends. First, for pure copper the resistivity increases with decreasing film thickness. Second, for the 100 nm films, the resistivity increases linearly with respect to oxygen percentage. Third, for 4.5 and 5 nm films, the addition of oxygen sharply decreases the resistivity to a minimum under conditions of 6 to 8% oxygen. All films below 10 nm thickness have the lowest resistivity for oxygen levels between 6 and 10%. Fourth, beyond 10% O<sub>2</sub>, the 4.5 and 5 nm film resistivity begins to linearly increase with oxygen content at a rate similar to that of the thicker films.

To clarify the origin of the resistivity reduction in thin Cu films, we have measured the roughness of the copper/cuprous oxide interface using x-ray reflectivity<sup>12,14</sup>. XRD was used to identify and quantify the concentration of the oxidation product (cuprous oxide) and to determine the Cu and Cu<sub>2</sub>O grain sizes. A film thickness of 10 nm was chosen because it is near the optimal thickness for X-ray reflectivity and is close to the thickness of practical interest. To corroborate these results, we have also studied the microstructure of 50 nm Cu films grown under similar conditions. Figure 2 shows reflectivity curves for four oxygen doping levels plotted as a function of the scattering vector Q. The film thickness determines the spacing between oscillation fringes, while the decay of the amplitude of the fringes with increasing Q is determined by the film roughness. Since the fringes extend to higher Q for the 10% oxygen film compared with the un-doped film (0.5 compared to 0.4 Å<sup>-1</sup>, respectively), the 10% film is smoother. To quantify the Cu-oxide/Cu roughness, the reflectivity data were fit to a multilayer Parratt model<sup>17</sup> with two layers: Cu film and surface Cu-oxide. The surface and oxide/Cu

roughnesses were fixed at the same value. Figure 3 shows the root-mean-squared (rms) Cu/Cu<sub>2</sub>O interface roughness extracted from the fits plotted as a function of oxygen concentration. The rms roughness of the copper/copper oxide interface is 1.2 nm in the un-doped film, drops to 0.7 nm at oxygen concentrations of 6 to 10%, then increases back to about 1.2 nm for high doping levels. The roughness minimum at 6-10% oxygen correlates well to the minimum in the resistivity data. This suggests that the reduced resistivity is due to increased specular scattering of the conduction electrons resulting from a smoothening of the Cu films.

Figure 4 shows XRD data taken on 10 nm Cu thin films, displaying intensity as a function of Q for several O<sub>2</sub> sputtering concentrations. Importantly, with increasing oxygen concentration the widths of the copper (111), (200), and (220) peaks increase (and hence the peak intensities drop), while the intensity of the Cu<sub>2</sub>O (111) peak rises. This shows that with increasing oxygen the Cu grain size decreases and Cu<sub>2</sub>O forms. The Cu<sub>2</sub>O present in the 0% film is the result of a thin surface oxide. We have estimated the Cu<sub>2</sub>O concentration from the ratio of the integrated intensities of the Cu (111) and the Cu<sub>2</sub>O (111) peaks (normalized for the scattering strengths of Cu(111) and Cu<sub>2</sub>O(111)). Since we are interested in the Cu<sub>2</sub>O in the Cu film, we have subtracted off the surface Cu<sub>2</sub>O (obtained from the 0% film). The cuprous oxide concentration is small for <10% O<sub>2</sub>, but increases significantly for >15% oxygen. Similar results hold for the 50 nm Cu films.

To determine the Cu and Cu<sub>2</sub>O grain sizes, the XRD data were fit to a model where the diffraction peak shapes contain contributions from nonuniform strain and grain size broadening<sup>15</sup>. The nonuniform strain contribution was assumed Gaussian, while the size broadening was assumed to originate from a lognormal distribution of grain sizes using an approximation given by Popa and Balzar<sup>16</sup>. Figure 5 shows the best fit copper and cuprous oxide grain diameters as a function of oxygen concentration. As is evident, the Cu grain size decreases by about a factor of two as the O<sub>2</sub> concentration is increased.

Cuprous oxide grains are small, approximately 2 nm, independent of oxygen concentration. Similar results hold for 50 nm Cu films.

From the Cu peak positions, we have calculated the lateral Cu lattice parameter as a function of oxygen gas composition. We find, remarkably, that the lattice parameter is independent of oxygen flow (3.622 and 3.623 Å for 10 and 50 nm films, respectively). This indicates that with increasing oxygen flow the oxygen does not form interstitials in the Cu (since this would increase the lattice parameter) and that all the oxygen is incorporated into the Cu as Cu<sub>2</sub>O.

These results shed light on the mechanism of resistance reduction due to growth of the Cu films in oxygen under our growth conditions. The sharp decrease in resistivity at 6-10% oxygen concentration is due to a reduction in the Cu/Cu<sub>2</sub>O interface roughness which is likely results in an increase in specular scattering of electrons at this interface. This reduction in interface roughness is a result, in turn, of a reduction in Cu grain size; we believe that the small Cu<sub>2</sub>O grains that form during growth in oxygen limit the growth of the Cu grains. Growth of the Cu film in more than 10% oxygen results in too much cuprous oxide formation, which increases the film resistivity (Cu<sub>2</sub>O is an insulator).

In summary, ion-beam sputtering of copper in a partial atmosphere of oxygen is an effective means to reduce Cu thin film resistivity. For minimal resistivity the optimum oxygen concentration is in the range of 6 to 10% O<sub>2</sub> under our sputtering conditions. The presence of fine cuprous oxide particles in the Cu creates a fine grain microstructure with a smoother interface that reflects conduction electrons instead of diffusely scattering them. The resulting increase of the mean free path of specularly scattered electrons decreases the resistivity.

This study was supported by IBM Almaden Research Center in conjunction with San José State University under National Science Foundation grant CHE-9625628. This research was carried out in

part at the National Synchrotron Light Source, Brookhaven National Laboratory, which is supported by the U.S. Department of Energy, Division of Materials Sciences and Division of Chemical Sciences, under Contract No. DE-AC02-98CH10886. Portions of this research were carried out at the Stanford Synchrotron Radiation Laboratory, a user facility operated by Stanford University on behalf of the U.S. Department of Energy, Office of Basic Energy Sciences.

---

### Figure Captions

Figure 1. Copper film resistivity as a function of O<sub>2</sub> percentage showing a sharp decrease of resistivity for 4.5 and 5 nm films (solid diamonds and solid squares, respectively) to a minimum at 6 to 10 % O<sub>2</sub>. The solid triangles are for 10 nm films and the solid circles are for 100 nm films. The oxygen percentage refers to the percent of oxygen flow relative to the sputtering gas flow. The lines are guides to the eye.

Figure 2. Cu/Cu<sub>2</sub>O interface X-ray reflectivity data for 10 nm Cu films sputtered with 0, 6, 10 and 30% O<sub>2</sub>. Lines are fits to the data. For clarity, the curves are offset along the vertical axis.

Figure 3. Copper/cuprous oxide interface roughness as a function of oxygen sputtering concentration showing a minimum at 6 to 10 % O<sub>2</sub>. The line is an eye guide.

---

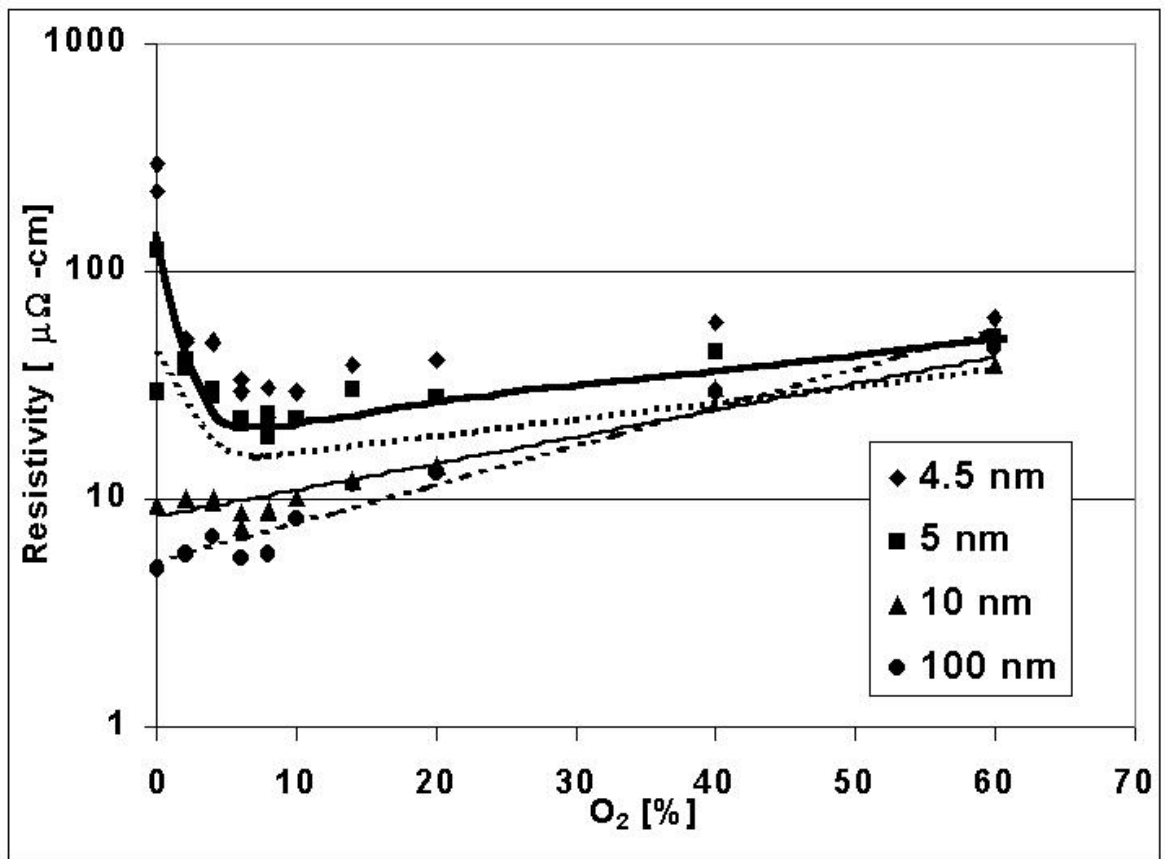
Figure 4. X-ray diffraction of 10 nm Cu films sputtered with six different O<sub>2</sub> percentages with Miller indices identifying the Bragg peaks. For clarity, each curve is offset along the vertical axis.

Figure 5. Cu and Cu<sub>2</sub>O grain diameter as a function of O<sub>2</sub> showing a two-fold reduction in Cu grain size (squares), while cuprous oxide (diamonds) is constant. The lines serve as guides to the eye.

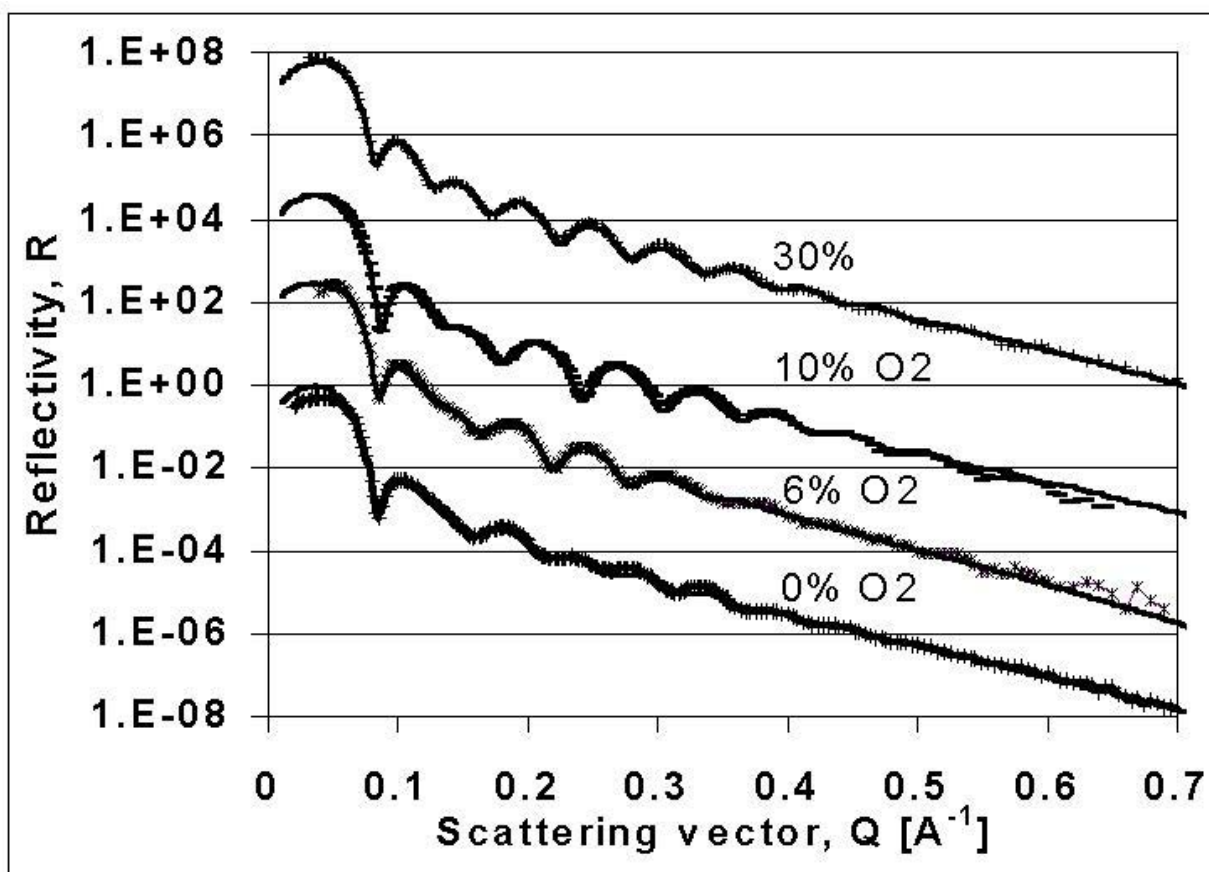
## References

- 1) R.L. Comstock, *J Mater Scie: Mater. in Electron.* **13** 509 (2002).
- 2) W.E. Bailey, C. Fery, K. Yamada and S.X. Wang, *J. Appl. Phys.* **85** (10), 7345 (1999).
- 3) S.X. Wang, K. Yamada and W.E. Bailey, *IEEE Internat. Magn. Conf. Proc. C-01* (2000).
- 4) W.Y. Lee, M. Carey, M.F. Toney, P. Rice, B. Gurney, H.-C. Chang, E. Allen and D. Mauri, *J. Appl. Phys.* **89** (11), 6925 (2001).
- 5) Z. Diao, Y. Huai and L. Chen, *J. Appl. Phys.* **91** (10), 7104 (2002).
- 6) A. Al-Jibouri, M. Hoban, Z. Lu and G. Pan, *J. Appl. Phys.* **91** (10), 7104 (2002).
- 7) D.J. Larson, A.K. Petford-Long, A. Cerezo, S.P. Bozeman, A. Morrone, Y.Q. Ma, A. Georgalakis and P.H. Clifton, *Phys. Rev. B* **67**, 144420 (2003).
- 8) K. Li, G. Han, J. Qiu, P. Luo, Z. Guo, Y. Zheng, and Y. Wu, *J. Appl. Phys.* **93** (10), 7708 (2003).
- 9) W.F. Egelhoff, C.J. Powell, R.D. McMichael, A.E. Berkowitz, , *J. Vac. Scie Technol. B* **17** (4), 1702 (1999).
- 10) W.F. Egelhoff, P.J. Chen, C.J. Powell, M.D. Stiles, R.D. McMichael, J.H. Judy, K. Takano, and A.E. Berkowitz, *J. Appl. Phys.* **82** (12), 6142 (1997).

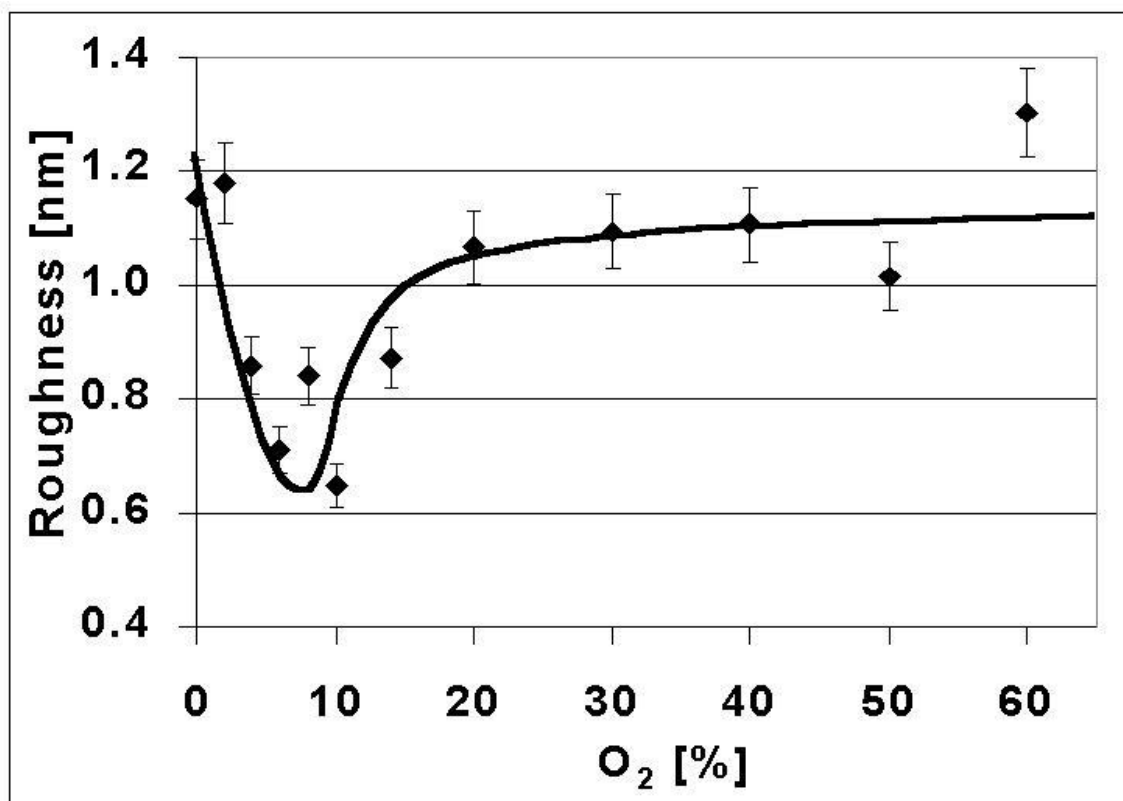
- 
- 11) S. Miura, M. Tsunoda, and M. Takahashi, *J. Appl. Phys.* **89** (11), 6308 (2001).
  - 12) C.M. Mate, B.K. Yen, D.C. Miller, M.F. Toney, M. Scarpulla and J.E. Frommer, *IEEE Trans. Magn.* **36** (1) 110 (2000).
  - 13) M.F. Toney, W.Y. Lee, J.A. Hedstrom, A. Kellock, *J. Appl. Phys.* **93** (12), 9902 (2003).
  - 14) V. Holy, U. Pietsch, T. Baumbach, *High resolution X-ray Scattering from Thin Films and Multilayers*, (Springer, Berlin, 1992).
  - 15) B.E. Warren, *X-ray Diffraction*, (Dover Publications, Reading Mass., 1969).
  - 16) N.C. Popa and D. Balzar, *J. Appl. Cryst.* **35**, 338-346 (2002).



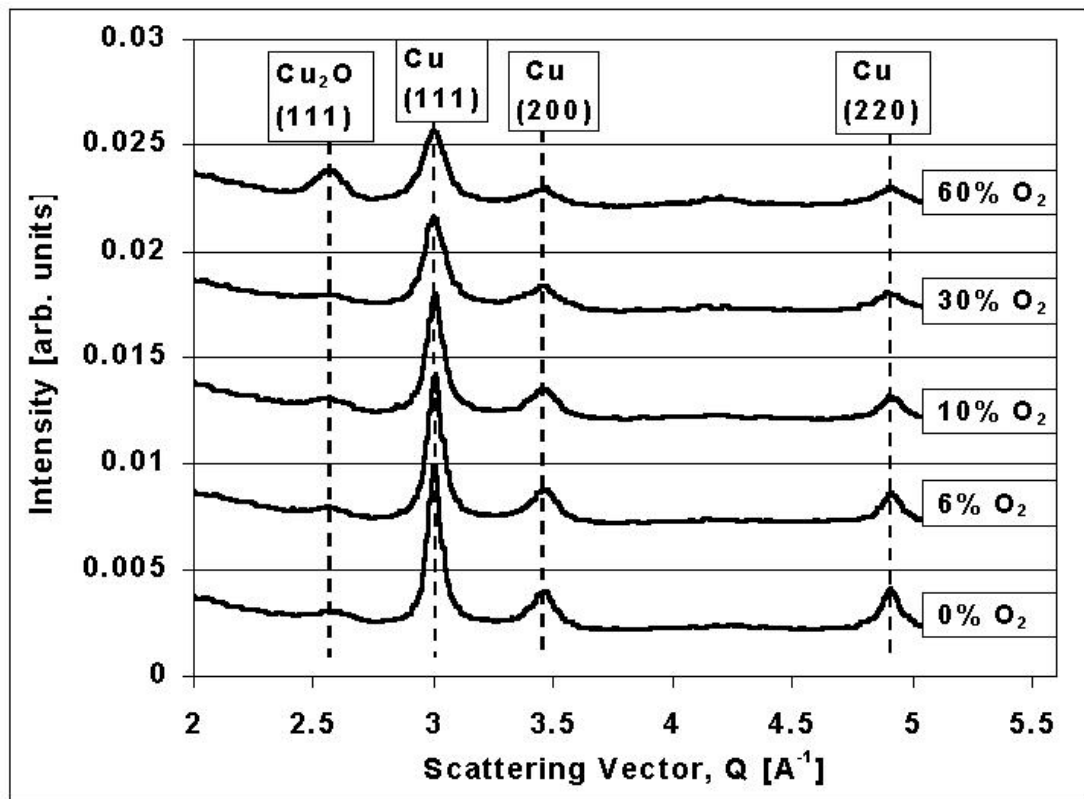
APL/Fig. 1 by Prater et al.



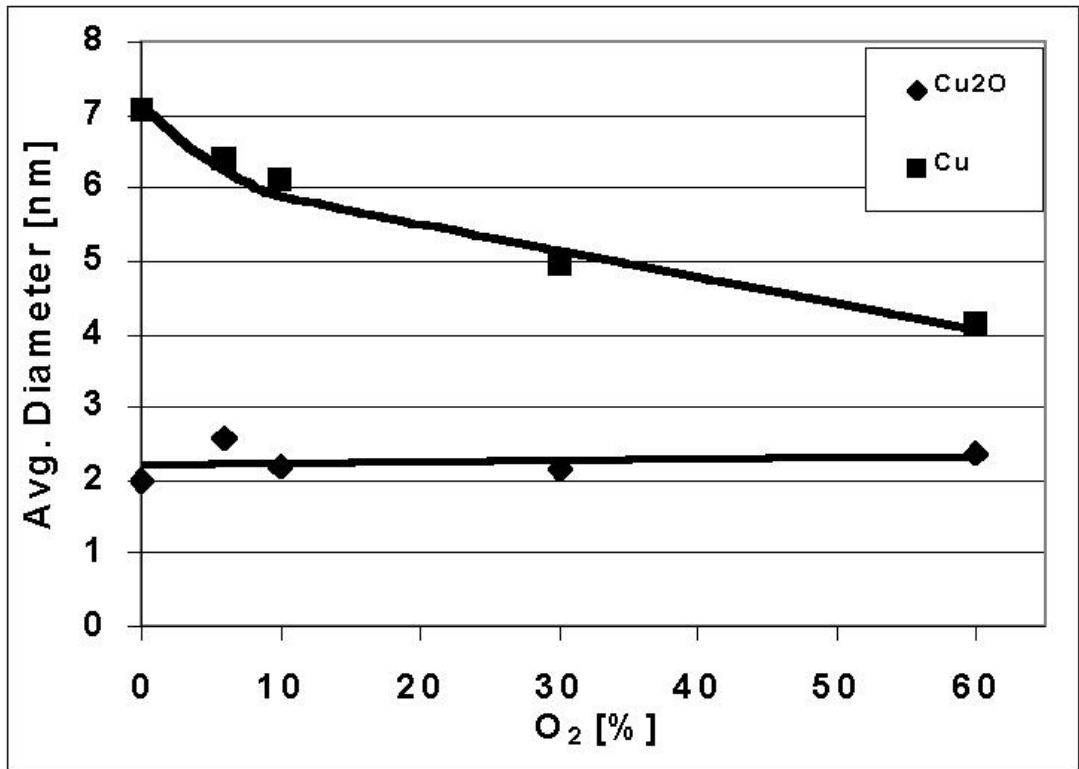
APL/Fig. 2 by Prater et al.



APL/Fig. 3 by Prater et al.



APL/Fig. 4 by Prater et al.



APL/Fig. 5 by Prater et al.